International Journal on Magnetic Particle Imaging
Vol 10, No 1, Suppl 1, Article ID 2403010, 4 Pages

Infinite Science Publishing

Proceedings Article

Extension of the Kaczmarz algorithm with a deep plug-and-play regularizer

Artyom Tsanda [a,b,*] · Paul Jürß [a,b] · Niklas Hackelberg [a,b] · Mirco Grosser [a,b] · Martin Möddel [a,b] · Tobias Knopp [a,b]

[a] Section for Biomedical Imaging, University Medical Center Hamburg-Eppendorf, Hamburg, Germany
[b] Institute for Biomedical Imaging, Hamburg University of Technology, Hamburg, Germany
[*] Corresponding author, email: artyom.tsanda@tuhh.de

Abstract

The Kaczmarz algorithm is widely used for image reconstruction in magnetic particle imaging (MPI) because it converges rapidly and provides good image quality even after a few iterations. It is often combined with Tikhonov regularization to cope with noisy measurements and the ill-posed nature of the imaging problem. In this abstract, we propose to combine the Kaczmarz method with a plug-and-play (PnP) denoiser for regularization, which can provide more specific prior knowledge than handcrafted priors. Using measurement data of a spiral phantom, we show that Kaczmarz-PnP yields excellent image quality, while speeding up the already fast convergence. Since the PnP denoiser is not coupled to the imaging operator, the Kaczmarz-PnP method is very generic and can be used for image reconstruction independently of the measurement sequence and MPI tracer type.

I. Introduction

Image reconstruction in magnetic particle imaging (MPI) is a challenging task because the reconstruction problem is ill-posed, and thus noise in the measurements is strongly amplified if not taken into account during reconstruction.

The standard approach to cope with measurement noise and system imperfections is to use a regularized least-squares approach, where the regularization function allows to incorporate prior knowledge about the particle concentration. Popular priors are the l_2 prior [1] and the sparsity promoting l_1 prior. The latter is often combined with a total variation prior [2, 3] to obtain smooth images. In case of dense objects, one can also apply the l_1-prior in the wavelet domain [4]. As these priors penalize image characteristics rather indirectly and often neglect many of the structural correlations present in MPI images, their denoising capabilities are limited.

In recent publications, the limitations of handcrafted regularizers were addressed using deep neural networks (DNN). These enable the incorporation of prior knowledge, e.g., by using a post-processing network [5, 6] or a deep image prior [7]. Another highly promising approach is to replace the proximal map of classical regularization functions by a learned denoiser based on a DNN. In MPI, this plug-and-play (PnP) approach was first combined with the alternating direction method of multipliers (ADMM) [8, 9]. Later on, this approach was further improved by incorporating a pre-trained denoiser and a learned data consistency condition into the optimization pipeline, which was then trained as a deep equilibrium model [10]. In both cases, the results demonstrated superior image quality but also relied on a large number of iterations to achieve convergence.

In this work, we propose to combine the PnP approach with the widely adopted Kaczmarz method for MPI image reconstruction. Notably, the Kaczmarz method is known to converge rapidly, due to the rows of the MPI system matrix being close to orthogonal [1]. The results of our experiments indicate that the Kaczmarz method retains its fast convergence when combined with a PnP denoiser. At the same time, the image quality provided by the Kaczmarz-PnP method is on par with that obtained by our implementation of the ADMM-PnP method proposed in [8].

II. Methods and Materials

The MPI imaging equation can be formulated in discrete form as

$$\boldsymbol{S}\boldsymbol{c}+\boldsymbol{\eta}=\boldsymbol{u} \tag{1}$$

where $\boldsymbol{S}\in\mathbb{C}^{M\times N}$ is the system matrix, $\boldsymbol{u}\in\mathbb{C}^{M}$ are the measurements, $\boldsymbol{\eta}\in\mathbb{C}^{M}$ is noise and $\boldsymbol{c}\in\mathbb{C}^{N}$ is the unknown particle concentration that we want to reconstruct. Usually, several operations, such as a weighting matrix and frequency filtering, are applied to the imaging equation prior to image reconstruction, and we assume them to be already included in (1).

The Kaczmarz algorithm allows solving linear systems of equations using a row-wise fixed-point iteration based on the successive over relaxation method [1]. To solve ill-posed problems, one can introduce l_2-regularization and apply the Kaczmarz iteration to the equation

$$\begin{pmatrix}\boldsymbol{S} & \lambda^{\frac{1}{2}}\boldsymbol{I}_M\end{pmatrix}\begin{pmatrix}\boldsymbol{c}\\ \boldsymbol{\nu}\end{pmatrix}=\boldsymbol{u}, \tag{2}$$

which leads to the iteration displayed in lines 3-6 of Algorithm 1. Furthermore, additional regularization in the form of projections or a more general proximal mapping can be applied after each outer Kaczmarz iteration [4].

Motivated by recent work [8], we suggest to apply a Gaussian denoiser $f^{\text{pp}}(\boldsymbol{c}):\mathbb{R}^N\to\mathbb{R}^N$ after each outer iteration. As the particle concentration may vary significantly, we scale it to $[0,1]$ using a min-max transformation. An overview of the complete Kaczmarz-PnP algorithm is provided in Algorithm 1.

We use 2D measurements of a spiral phantom for reconstruction. Frequencies are filtered with an SNR threshold of 1.5 and weighted to realize noise whitening [11]. We compare Kaczmarz-PnP with the regular l_2-regularized Kaczmarz method and with a ADMM-PnP. The latter is similar to the one from [8] but penalizes the commonly used l_2-norm of the residual to enforce data consistency. For Kaczmarz-PnP we set the Tikhonov regularization parameter λ to zero, for Kaczmarz-l_2 λ equals 0.05. We use the original PnP denoiser [8], which was trained to denoise simulated vessel phantoms and is agnostic of the given reconstruction algorithm. All reconstructions used 150 iterations and were performed using the Julia package RegularizedLeastSquares.jl[1].

[1] https://github.com/JuliaImageRecon/RegularizedLeastSquares.jl.

Algorithm 1 Pseudo code of the Kaczmarz-PnP algorithm applied to the regularized least-squares problem.

Input:	$\boldsymbol{S}\in\mathbb{C}^{M\times N}$,	system matrix
	$\boldsymbol{u}\in\mathbb{C}^{M}$,	measurements
	$\boldsymbol{c}^{(1)}\in\mathbb{C}^{N}$,	initial guess
	$N^{\text{iter}}\in\mathbb{N}$,	number of iterations
	f^{pp},	pretrained PnP denoiser
	$\mathcal{S}$,	min-max scaling
	$\lambda\geq 0$	regularization parameters

1: $\boldsymbol{\nu}=\boldsymbol{0}$
2: **for** $l=1,2,\dots,N^{\text{iter}}$ **do**
3: **for** $k=1,2\dots,M$ **do**
4: $\boldsymbol{c}^{(l)}\leftarrow\boldsymbol{c}^{(l)}+\dfrac{u_k-\langle\boldsymbol{s}_k^*,\boldsymbol{c}^{(l)}\rangle-\lambda^{\frac{1}{2}}\nu_k}{\|\boldsymbol{s}_k\|_2^2+\lambda}\boldsymbol{s}_k^*$
5: $\nu_k\leftarrow\nu_k+\dfrac{u_k-\langle\boldsymbol{s}_k^*,\boldsymbol{c}^{(l)}\rangle-\lambda^{\frac{1}{2}}\nu_k}{\|\boldsymbol{s}_k\|_2^2+\lambda}\lambda^{\frac{1}{2}}$
6: **end for**
7: $\boldsymbol{c}^{(l)}\leftarrow P_+(\boldsymbol{c}^{(l)})$ projection onto $\mathbb{R}^+$
8: $\boldsymbol{c}^{(l)}\leftarrow\mathcal{S}^{-1}\left(f^{\text{pp}}\left(\mathcal{S}\left(\boldsymbol{c}^{(l)}\right)\right)\right)$
9: **end for**

Output: $\boldsymbol{c}^{(N^{\text{iter}})}\in\mathbb{C}^{N}$ solution

To quantitatively analyze convergence properties, we calculate the normalized root mean squared error (NRMSE) between each intermediate and the final $\boldsymbol{c}$. We consider a method to be converged at a certain iteration if the corresponding value of the NRMSE is less than $\varepsilon=10^{-2}$. As the ground truth is not available, the described method does not take into account the accuracy of the final reconstruction for the convergence analysis. Additionally, we provide visual results along with a photo of the phantom.

III. Results

The iterative progress of the considered algorithms is shown exemplarily for the spiral phantom in Figure 1. Both quantitative and visual results indicate faster convergence for the Kaczmarz-PnP algorithm which converges already after the fourth iteration. The final image produced by Kaczmarz PnP demonstrates less artifacts compared to Kaczmarz-l_2. The results of Kaczmarz-PnP and ADMM-PnP differ at the upper-left corner of the phantom which is missing for Kaczmarz methods. The ADMM-PnP leads to a more homogeneous particle concentration along the spiral but also shows implausible particle concentrations in the upper left corner. The center of the spiral is reconstructed accurately, demonstrating comparable image quality for both algorithms.

10.18416/ijmpi.2024.2403010

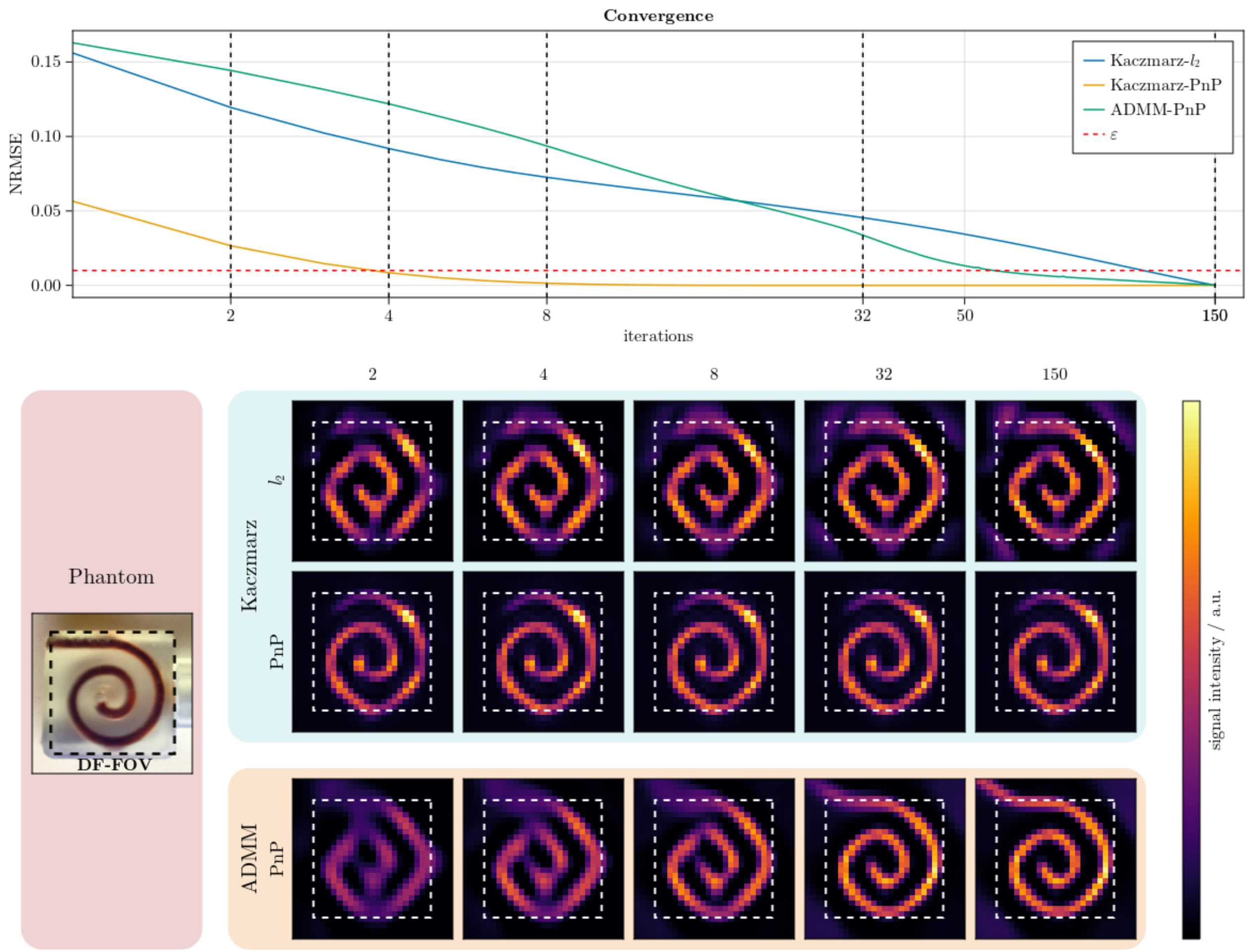

Figure 1: The progress of image reconstruction. A spiral phantom was reconstructed using Kaczmarz-l_2, Kaczmarz-PnP and ADMM-PnP algorithms. The upper plot shows the NRMSE of each iteration compared to the final iteration along with the defined convergence criterion (ε). The intermediate results of image reconstruction after iterations 2, 4, 8, 32 and 150 are showed below. The images are normalized by the corresponding maximum concentration. The drive-field field of view is marked by dashed boxes.

IV. Discussion and Conclusion

In this work, we propose to combine the Kaczmarz algorithm with a plug-and-play denoiser. Our results indicate that this combination is very effective and enables high-quality image reconstruction while requiring only a few iterations for convergence.

Nevertheless, we note that our experiments only show the methods potential in a very limited setting. A more rigorous evaluation on different datasets and a comparison to a larger set of methods (including PP-MPI [8] and DEQ-MPI [8]) is needed to more precisely delineate the strengths and limitations of the Kaczmarz-PnP method. Additionally, the min-max scaling introduced in this paper to address the issue of variable particle concentration may not be optimal for certain applications that demand consistency between independent reconstructions, such as time-series data of a particle bolus. For these cases, the scaling should be global, *i.e.*, shared across reconstructions. Finally, a further improvement might be achievable by studying different denoiser architectures.

Acknowledgment

This project is funded by the Deutsche Forschungsgemeinschaft (DFG, German Research Foundation) – SFB 1615 – 503850735.

References

[1] T. Knopp, J. Rahmer, T. F. Sattel, S. Biederer, J. Weizenecker, B. Gleich, J. Borgert, and T. M. Buzug. Weighted iterative reconstruction for magnetic particle imaging. *Physics in Medicine & Biology*, 55(6):1577, 2010.

[2] M. Storath, C. Brandt, M. Hofmann, T. Knopp, J. Salamon, A. Weber, and A. Weinmann. Edge preserving and noise reducing reconstruction for magnetic particle imaging. *IEEE Transactions on Medical Imaging*, 36(1):74–85, 2016.

[3] S. Ilbey, C. B. Top, A. Güngör, T. Çukur, E. U. Saritas, and H. E. Güven. Comparison of system-matrix-based and projection-based reconstructions for field free line magnetic particle imaging. *International Journal on Magnetic Particle Imaging*, 3(1), 2017.

[4] F. Lieb and T. Knopp. A wavelet-based sparse row-action method for image reconstruction in magnetic particle imaging. *Medical physics*, 48(7):3893–3903, 2021.

[5] Y. Shang, J. Liu, L. Zhang, X. Wu, P. Zhang, L. Yin, H. Hui, and J. Tian. Deep learning for improving the spatial resolution of magnetic particle imaging. *Physics in Medicine & Biology*, 67(12):125012, 2022.

[6] T. Knopp, P. Jürß, and M. Grosser. A deep learning approach for automatic image reconstruction in mpi. *International Journal on Magnetic Particle Imaging*, 9(1, suppl. 1), 2023.

[7] S. Dittmer, T. Kluth, M. T. R. Henriksen, and P. Maass. Deep image prior for 3D magnetic particle imaging: A quantitative comparison of regularization techniques on Open MPI dataset. *International Journal on Magnetic Particle Imaging*, 7(1), 2021.

[8] B. Askin, A. Güngör, D. Alptekin Soydan, E. U. Saritas, C. B. Top, and T. Cukur, PP-MPI: A deep plug-and-play prior for magnetic particle imaging reconstruction, in *International Workshop on Machine Learning for Medical Image Reconstruction*, Springer, 105–114, 2022.

[9] A. Güngör, B. Aşkın, D. A. Soydan, E. U. Saritas, C. B. Top, and T. Çukur. A denoiser scaling technique for plug-and-play MPI reconstruction. *International Journal on Magnetic Particle Imaging*, 9(1 Suppl 1), 2023.

[10] A. Güngör, B. Askin, D. A. Soydan, C. B. Top, E. U. Saritas, and T. Çukur. DEQ-MPI: A deep equilibrium reconstruction with learned consistency for magnetic particle imaging. *IEEE Transactions on Medical Imaging*, 2023.

[11] T. Kluth and B. Jin. Enhanced reconstruction in magnetic particle imaging by whitening and randomized SVD approximation. *Physics in Medicine & Biology*, 64(12):125026, 2019.

10.18416/ijmpi.2024.2403010